JOURNAL OF KUFA–PHYSICS
www.uokufa.edu.iq/journals/index.php/jkp | ISSN: 2077–5830

Fabrication and Characterization of Dye Sensitized Solar Cells Based on TiO_2

Ghufran M. Abbas ***Aref S. Baron**

Department of Physics, Faculty of Sciences, University of Kufa, Iraq.

Corresponding Author E-mail: arif.aljuburi@uokufa.edu.iq

ARTICLE INF

Article history:
Received: 17 NOV, 2020
Revised: 23 MAR, 2021
Accepted: , 1 APR, 2021
Available Online: 6 JUN, 2021

Keywords:

TiO_2
Hydrothermal method
Solar cell
Dye Sensitized.

ABSTRACT

Thin films of TiO_2 nanostructures were prepared on FTO bases with different temperatures 140 ° C and 160 °C for 4 h. The XRD results showed that that there was an increase in the intensity of the peaks of the prepared (quadrangular) samples and a decrease in the FWHM was observed due to the increase in temperature as well as increase in the grain size in which the distance between the grains was decreased. According to the UV-Vis results, the energy band gap E_g was calculated from the reflectivity spectrum using the Kobelka - Monk equation. The increase in temperature has reduced the energy band gap, which shifting it towards the blue direction. FESEM, an increase in the surface thickness of the thin film due to an increase in the preparation temperature. The solar cell efficiency was decreased with increased in temperature. Where it was found the efficiency reduce rom 0.17% to 0.004% for As for 140 ° C and 160 ° C respectively.

DOI: >>>

تحضير وتوصيف خلايا شمسية صبغية على اساس من ثنائي اوكسيد التيتانيوم

غفران مفيد عباس **عارف صالح بارون**

قسم الفيزياء – كلية العلوم – جامعة الكوفة.

الـــخُـــلاصـــة

تم تحضير أغشية رقيقة من الهياكل النانوية لثنائي اوكسيد التيتانيوم على قواعد *FTO* بدرجات حرارة مختلفة ١٤٠ درجة مئوية و ١٦٠ درجة مئوية لمدة ٤ ساعات. أظهرت نتائج *XRD* أن هناك زيادة في شدة القمم للعينات المحضرة (رباعي الزوايا) ولوحظ انخفاض في منتصف عرض القمة *FWHM* بسبب الزيادة في درجة الحرارة وكذلك زيادة الحجم الحبيبي حيث انخفضت المسافة بين الحد الحبيبي . وفقًا لنتائج *UV-Vis* ، تم حساب فجوة نطاق الطاقة *Eg* من طيف الانعكاسية باستخدام معادلة *Kobelka - Monk*.أدت الزيادة في درجة الحرارة إلى تقليل فجوة نطاق الطاقة ، مما أدى إلى تحويلها نحو الاتجاه الأزرق. بينت صور

الكلمات المفتاحية:

ثنائي اوكسيد التيتانيوم
الانماء المائي
الخلايا الشمسية
الصبغات الحساسة

FESEM ، زيادة في سمك السطح للفيلم الرقيق بسبب زيادة درجة حرارة التحضير. انخفضت كفاءة الخلايا الشمسية مع زيادة درجة الحرارة. حيث وجد أن الكفاءة تنخفض بنسبة ١٧.٠٪ إلى ٠.٠٠٤٪ بالنسبة لـ ١٤٠ درجة مئوية و ١٦٠ درجة مئوية على التوالي.

1. INTRODUCTION

The energy produced around the world uses fossil fuels. This fuel is harmful to the environment because it emits carbon dioxide and drains fossil fuels around its sustainable use for future energy needs[1] . The sun is one of the largest and most important sources of energy in life on earth and is considered a source of all types of energy. The solar energy that the sun radiates 3×1024 J per year, which is equivalent to ten times the current demand for energy[2, 3]

Sun energy is divided into two parts according to its uses: systems that convert solar radiation into thermal energy called thermal photovoltaic systems, and devices that convert solar energy into electrical energy are called solar cells or photovoltaics [٤].In 1991 Dye sensitized solar cell were first developed by B. O'Regan and M. Grätze. Dye solar cells are a cost-effective way to convert photon energy into electrical energy. Here dye is used to absorb visible light. Every color has it the wavelength range that absorbs light excludes this range from the wave length Therefore, it is easy to convert the energy of a photon [5].

After that, DSSC attracted many researchers because it is low cost easy to manufacture, non-toxic and environmentally friendly Operation. The efficiency of DSSCs has reached 11.20%[6], Over the past decades they have done extensive research on photocatalys is for applications of titanium dioxide. It is used in photovoltaics [7] and it is used in water purification systems [8]

as well as in sterilization and self-cleaning [9]and because it is considered inexpensive, thin films have been used in a wide range of fields. The energy of titanium dioxide varies according to its structure [10]The energy gap of the anatase phase is 3.5 eV while the rutile phase is 3.0-3.2 eV [11] The rutile phase absorbs light in a wide range of wavelengths, so it is considered better than performing anatase, but the photocatalysis of anatase is higher due to its high density. Therefore, attention has been paid to understanding the anatase-phase photostimulation [12, 13]

There are different techniques that have been used in the manufacture of thin films, including the sol-gel, the hydrothermal method [14]the spin coating, and the chemical precipitation method [15]

2. Preparation of Dye-Sensitized Solar Cell (DSSC)

DSSC mainly consists of three parts as dye sensitivity TiO_2 film deposited on FTO glass substrate, electrolytes and Carbon counter electrode. First mix 2 mL (TiCl4) with 8 mL of butanol. TiCl4 was placed in a three-neck flask. Butanol was added drop by drop using a magnetic stirrer applied without heating to the butanol end and the fog clears. The oiled yellow solution was obtained. In a glass container, the solution consisting of (12.5) ml of distilled water is mixed with (12.5) ml of hydrochloric acid at a concentration of (35.4%) and left for 15 minutes, then placed (0.3) ml of TTB and left for 25 minutes. Mixing is done with a Teflon magnetic stirrer, the FTO is placed at a certain angle and then the solution is added to cover the sample, leaving a distance from the top where this portion is conductive for the measurement. Then the autoclave container is tightly closed and placed in the oven at temperatures of (140,160) ° C for four hours, then the hydrothermal reactor is cooled to room temperature. Then she will give birth at 400 ° C for half an hour.

Dye preparation: (0.0235) methyl violet 10b is added to (15) ml of ethanol and mixed. Well, by using a magnetic stirrer for (15) minutes at room temperature, leaving it for a while and immersing the prepared samples in the dye for 24 hours before the measurement

(1.5609) of Na_2S with (0.6413) of S with (0.6567) of KCl is added to a beaker containing (7ml) ethanol with (3ml) of distilled water and mixed for one hour at room temperature to the preparation of the electrolyte solution by using a

magnetic stirrer until it is dissolved. Leave it on for 24 hours before using it. Then an amount of carbon is added to the another FTO glass bases using the adhesive method to prepper the anode. After that, it is heat treated for 15 seconds at 300 ° C in order to provide more adhesion to the FTO base surface

3. RESULTS AND DISCUSSION

Figure (1) illustrates Refers to the sample diffraction pattern S1(TiO_2 prepared on a FTO base by HIP method at 140 temperature for 4 h with annealing) where diffraction peaks indicate (101), (004), (200), (213), (204) anatase phase also at 2θ = (26.59), (37.85), (51.63), (61.86), (65.71) uniformity of the cell network constant (a = b = 3.5372 Å) and (c = 9.4979 Å) the corresponds to [16] Figure (2) indicates the diffraction pattern of sample S2 (TiO_2 prepared on a FTO base by HIP method at 160 temperature for 4 h with annealing) , where the diffraction peaks (101), (103) (004), (200), (213) (204) indicate anatase phase also in (26.46)), (35.92) (37.58), (51.3), (61.54), (65.36), the unified network constant of S2 is (a = b = 4.6540 Å) and (c = 9.5656 Å) These results correspond to the card profile(JCPDS-04-0477).

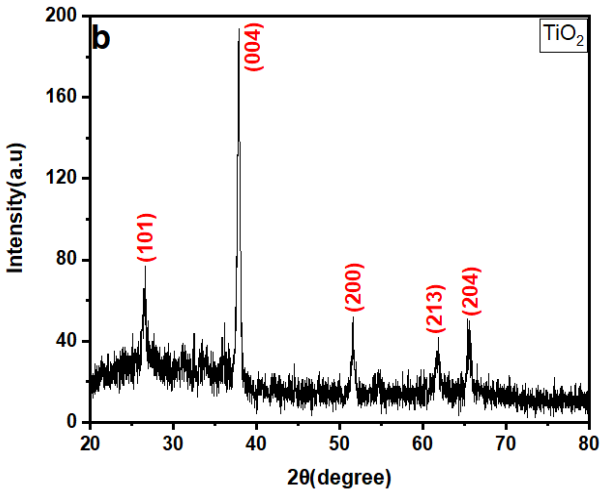

Fig. (1)XRD for S1 for 140 ° C under annealing.

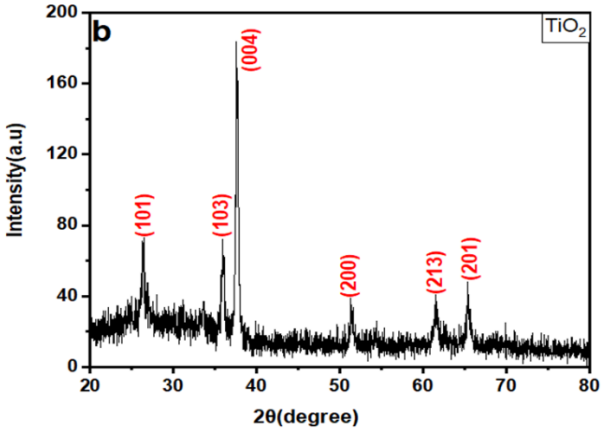

Fig. (2)XRD for S2 for 160 ° C under annealing.

When comparing these samples with greater diffusion activation energy, thus it will allow the lower energy atoms to move to the appropriate location in the crystal structure ,thus the crystals will grow in their preferred direction and then the crystal fusion process will start to form larger granules and within the grain boundaries, the oxygen defects will decrease. An increase in temperature leads to an increase in the profile size and an increase in the grain size and thus the surface roughness increases and also the intensity of the peaks as shown by the XRD patterns will become narrow[16, 17].

Table (1). Data on thin TiO_2 films at different temperatures with with annealing.

Sample	D (nm)	δ (nm^{-2})	ε
S1	31.738	0.00123	0.0012
S2	24.121	0.00201	0.0015

The energy band gap was calculated by the Kubelka-Munk method based on the reflectivity spectrum $(\alpha = F(R) = \frac{(1-R)^2}{2R})$ Figure (3) shows the reflection spectrum of TiO_2, in which the energy gap of sample S1 was calculated, which is equal to 3.38 eV .Figure (4) shows the spectrum of reflectivity at 160 ° C for sample S2 the energy gap began to decrease and shift towards the blue direction, so that the energy gap of sample S2 became 3.1 volts and these results are compatible with[18].

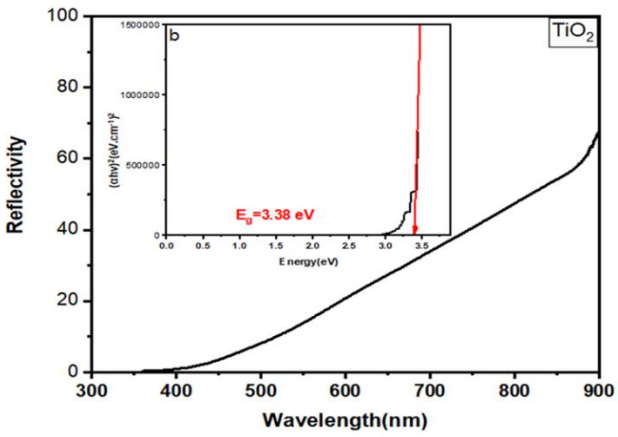

Fig. (3) The reflectivity spectrum of sample S1.

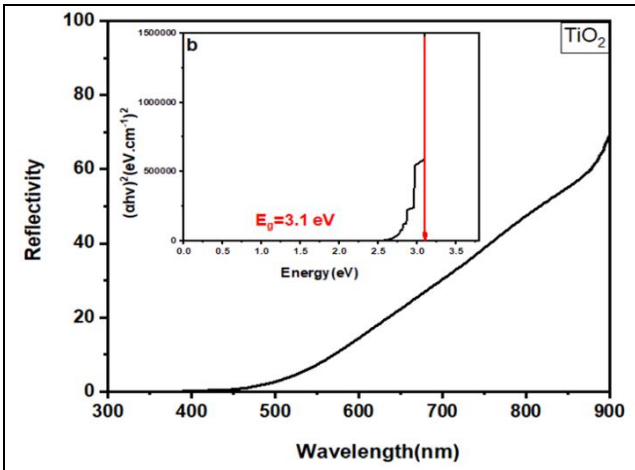

Fig. (4) The reflectivity spectrum of sample S2.

Figures (5) and (6) show the TiO2 formation that was grown at different temperatures of 140 and 160 ° C for four hours. The growth on the FTO was in nanorod form The growth of the sticks is perpendicular to the FTO, and the rod shape was quadrangular with square sides, there was a difference between the samples in terms of nanorod density and this is due to the increase in temperature in addition to the annealing temperature and the effect of temperature [18] on increasing the grain size and thus increasing the surface significantly

4. FESEM Measurement

Typical FESEM images show the TiO_2 formation that was prepared at different temperatures (140, and 160 ° C for four hours). The growth of TiO_2 on the FTO is in the nanorod form which shape is tetragonal with square sides. Figures 5 and 6 appeared that the samples S1 less density than S2, and this is due to the increase in preparation temperature [19, 20]. The effect of the temperature on the increase in the size of the grains and thus the surface increase significantly which leads to increase the crystallinity of the material and hence increases the number of crystallites [16].

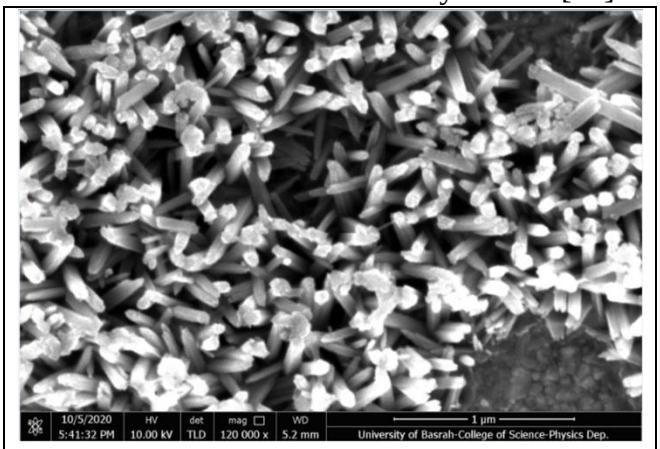

Fig. (5) FESEM to the sample S1.

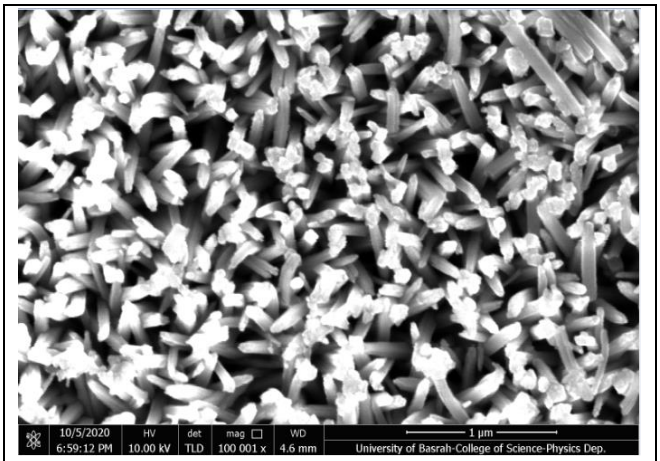

Fig. (6) FESEM to the sample S2.

5. Solar Cell Parameters

Solar cell coefficients were calculated using Keithly 2400. The intensity of the light source was equal to 100 mW which was simulated for sunlight as the filling factor was calculated from the equation

($FF = \frac{I_{mp} * V_{mp}}{I_{sc} * V_{oc}}$) The efficiency of the solar cell was also calculated from equation ($\eta = \frac{P_{out}}{P_{in}}$) for two samples with different temperatures

FF: Represents the fill factor

Ŋ: It represents the efficiency of the solar cell. By compared between the values of solar cell parameters for S1and S2 we found: all parameters increasing in S1 than S2. Voc=0.48mv, J_{SC}=0.1984 mA.cm^{-2}, FF= 9.27 and

the efficiency of the solar cell =0.17% for S1 sample. While these parameters decrease in S2 as shown in table1-2 where the efficiency about 0.0041%. This is due to the fact that the increase in nanorod density led to a decrease in absorbance as a result of the increase in grain size. Thus, this led to a decrease in charge carriers which led to a decrease in efficiency [21, 22].

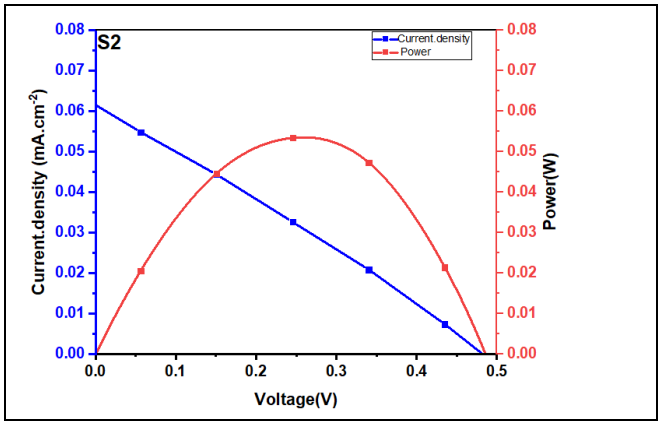

Fig. (7) J-V curve and P-V curve of S1 sample.

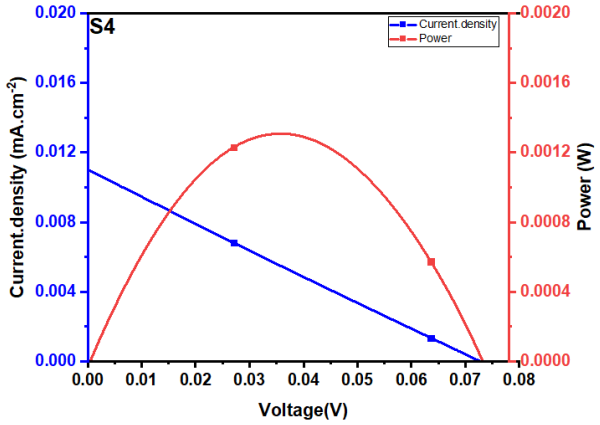

Fig. (8) J-V curve and P-V curve of S2 sample.

Table (2) Solar cell parameters for the sample S1 and S2

Sample	V_{OC} mV	J_{SC} mA.cm^{-2}	V_{MAX} mV	J_{MAX} mA.cm^{-2}	(Fill factor) FF %	(efficiency) ŋ %
S1	0.48	0.1984	0.90837	2.02933	9.27	0.17
S2	0.0715	0.725	0.90844	1.92321	3.37	0.0041

6. CONCLUSION

The temperature showed an effect on the grain size and distance between them, as well as the decrease in the energy gap. The highest efficiency was at the S1 sample of 140 ° C, which was equal to 0.17% and decreased to 0.004١% at S4 to 160 ° C.

7. ACKNOWLEDGMENT

This research is supported by the department of physics, faculty of Science, University of Kufa.

8. REFERENCES

[1] J. Khan, M.H. Arsalan, Solar power technologies for sustainable electricity generation–A review, Renewable and Sustainable Energy Reviews, 55 (2016) 414-425.

[2] C.K. Dyer, P.T. Moseley, Z. Ogumi, D.A. Rand, B. Scrosati, J. Garche, Encyclopedia of electrochemical power sources, Elsevier Science & Technology, 2009.

[3] U. Mehmood, M.Z. Aslam, R. Shawabkeh, I.A. Hussein, W. Ahmad, A.G. Rana, Improvement in Photovoltaic Performance of Dye Sensitized Solar Cell Using Activated Carbon-TiO 2 Composites-Based Photoanode, IEEE Journal of Photovoltaics, 6 (2016) 1191-1195.

[4] S.R. Kodigala, Cu (In1− xGax) Se2 and CuIn (Se1− xSx) 2 Thin Film Solar Cells, in: Thin Films and Nanostructures, Elsevier, 2010, pp. 505-679.

[5] V. Nandakumar, S. Suresh, C. Sreekala, S. Sudheer, V.M. Pillai, Hemigraphis colorata as a natural dye for solar energy conversion, Materials Today: Proceedings, 4 (2017) 4358-4365.

[6] R. Buscaino, C. Baiocchi, C. Barolo, C. Medana, M. Grätzel, M.K. Nazeeruddin, G. Viscardi, A mass spectrometric analysis of sensitizer solution used for dye-sensitized solar cell, Inorganica Chimica Acta, 361 (2008) 798-805.

[7] B. Lee, J. He, R.P. Chang, M.G. Kanatzidis, All-solid-state dye-sensitized solar cells with high efficiency, Nature, 485 (2012) 486-489.

[8] K. Nakata, A. Fujishima, TiO2 photocatalysis: Design and applications, Journal of photochemistry and photobiology C: Photochemistry Reviews, 13 (2012) 169-189.
[9] T. Kamegawa, Y. Shimizu, H. Yamashita, Superhydrophobic surfaces with photocatalytic self-cleaning properties by nanocomposite coating of TiO2 and polytetrafluoroethylene, Advanced Materials, 24 (2012) 3697-3700.
[10] T. Fuyuki, H. Matsunami, Electronic properties of the interface between Si and TiO2 deposited at very low temperatures, Japanese Journal of Applied Physics, 25 (1986) 1288.
[11] Q. Deng, X. Xia, M. Guo, Y. Gao, G. Shao, Mn-doped TiO2 nanopowders with remarkable visible light photocatalytic activity, Materials Letters, 65 (2011) 2051-2054.
[12] R.J. Tayade, P.K. Surolia, R.G. Kulkarni, R.V. Jasra, Photocatalytic degradation of dyes and organic contaminants in water using nanocrystalline anatase and rutile TiO2, Science and Technology of Advanced Materials, 8 (2007) 455.
[13] D.A. Hanaor, C.C. Sorrell, Review of the anatase to rutile phase transformation, Journal of Materials science, 46 (2011) 855-874.
[14] A. Nakaruk, D. Ragazzon, C. Sorrell, Anatase–rutile transformation through high-temperature annealing of titania films produced by ultrasonic spray pyrolysis, Thin Solid Films, 518 (2010) 3735-3742.
[15] V. Puddu, H. Choi, D.D. Dionysiou, G.L. Puma, TiO2 photocatalyst for indoor air remediation: Influence of crystallinity, crystal phase, and UV radiation intensity on trichloroethylene degradation, Applied Catalysis B: Environmental, 94 (2010) 211-218.
[16] C.-P. Lin, H. Chen, A. Nakaruk, P. Koshy, C. Sorrell, Effect of annealing temperature on the photocatalytic activity of TiO2 thin films, Energy Procedia, 34 (2013) 627-636.
[17] Z.-N. Ng, K.-Y. Chan, T. Tohsophon, Effects of annealing temperature on ZnO and AZO films prepared by sol–gel technique, Applied Surface Science, 258 (2012) 9604-9609.
[18] C. Cao, C. Hu, X. Wang, S. Wang, Y. Tian, H. Zhang, UV sensor based on TiO2 nanorod arrays on FTO thin film, Sensors and Actuators B: Chemical, 156 (2011) 114-119.
[19] R. Danish, F. Ahmed, N. Arshi, M. Anwar, B.H. Koo, Facile synthesis of single-crystalline rutile TiO2 nano-rods by solution method, Transactions of Nonferrous Metals Society of China, 24 (2014) s152-s156.
[20] M.A. Ghufran, S.B. Aref, STUDY EFFECT THE TEMPERATURE OF PREPARATION AND ANNEALING ON TIO2 CHARACTERIZATIONS, Theoretical & Applied Science, (2020) 284-290.
[21] M. Kamruzzaman, The effect of ZnO/ZnSe core/shell nanorod arrays photoelectrodes on PbS quantum dot sensitized solar cell performance, Nanoscale Advances, 2 (2020) 286-295.
[22] A. Al Mamun, Effect of Grain Size and Interface Engineering on the Photovoltaic Performance and Stability of Perovskite Solar Cells, in, Old Dominion University, 2019.